Journal of Materials Chemistry

Cite this: *J. Mater. Chem.*, 2011, **21**, 11708

www.rsc.org/materials

FEATURE ARTICLE

Recent progress of high performance organic thin film field-effect transistors

Qing Meng,[ab] Huanli Dong,*[a] Wenping Hu*[a] and Daoben Zhu[a]

Received 17th January 2011, Accepted 21st April 2011
DOI: 10.1039/c1jm10243e

During the past few decades, thousands of organic semiconductors have been designed and synthesized for organic thin-film transistors (OTFTs). However, most of them exhibit non-ideal performance. After carefully reviewing recent OTFTs with high performance, *e.g.*, OTFTs with mobility over 1.0 $cm^2 V^{-1} s^{-1}$, guidelines for device fabrication are highlighted, especially the importance in finding promising compounds and regulating molecular properties for OTFTs, as well as in modifying surfaces of dielectric and electrodes for high-quality devices.

Introduction

As an important branch of organic electronics, organic thin-film transistors (OTFTs) has aroused great attention for decades due to their potential application in cheap, large-scale and flexible organic electronics.[1–5] Various theories of molecular design based on abundant experience and experiments were established by synthesists.[6–9] Conjugated polymers and small molecular weight compounds (SMWCs) were favorable candidates for semiconducting materials,[10–16] wherein SMWCs were extensively developed due to their merits of convenient purification, uniform molecular weight and strong intermolecular interactions. On the other side, device researchers invented delicate techniques to improve device fabrication, in which interface engineering (such as chemical modification of dielectrics by self-assembled silane based monolayers,[17] and improvement of electrode/semiconductor interfacial interaction by alkanethiol stabilizer[18]) showed great potential in optimization of device performance.[19–21]

Top- and bottom-contact configurations (source and drain electrodes are on or below organic semiconducting layer) are generally adopted in OTFTs.[22] Doped silicon with a thermally grown layer of SiO_2 (200–500 nm thick) is widely used as a substrate in the scientific research of OTFTs. Although inorganic layers such as SiO_2 are sufficient to perform as a dielectric, there are so many silanol groups and other defects at its surface to trap carriers. Whereas organic dielectrics which could passivate the surface of SiO_2 by various functional groups are preferable. Some alkylsilanes (such as octadecyltrichlorosilane (OTS), hexamethyldisilazane (HMDS), *etc.*) and various polymers (such as polymethyl methacrylate (PMMA), parylene, cytop, *etc.*) are popular candidates for surface modification, providing a smoother surface of dielectric to induce high-quality organic semiconducting films. During the interface engineering,

[a]*Beijing National Laboratory for Molecular Sciences, Key Laboratory of Organic Solids, Institute of Chemistry, Chinese Academy of Sciences, Beijing, 100190, China. E-mail: huwp@iccas.ac.cn*
[b]*Graduate School of Chinese Academy of Sciences, Beijing, 100039, China*

Qing Meng

Qing Meng grew up in the Shanxi province, China. She received her B.S. degree (2004) at the School of Chemistry and Chemical Engineering, Shanxi University. Then she joined the Institute of Chemistry, Chinese Academy of Sciences. In 2006, she continued her study in the institute as a Ph.D candidate. She focuses on the design and synthesis of new organic semiconductors.

Huanli Dong

Huanli Dong is an assistant Professor at the Institute of Chemistry, Chinese Academy of Sciences (CAS). She grew up in the Shandong province, China. She received her Ph.D degree from the Institute of Chemistry, CAS in 2009 after she got her M. S. degree (2006) at the Fujian Institute of Research on the Structure of Material, CAS. She is presently focusing on molecular electronics including synthesis, preparation and characterization of organic/polymer materials and optoelectronic devices.

the dramatically decreased surface roughness and trap density were effective in reducing Schoktty contact, which was good for lowering the drive power of the device. At the same time, the surface energy could be directionally modified for compatibility of the electrode/dielectric with a semiconductor, improving molecular packing in an active layer and carrier injection between the electrode and the semiconductor.

Semiconducting films play a critical role in the field-effect behavior, wherein the well-known region to form a conductive channel is the semiconductor–dielectric interface.[23–26] There are two major categories of film fabrication. Vacuum-deposition as a traditional technique is extensively used in OTFTs. Although the fabrication needs rigorous condition such as high vacuum circumstance and accurate thickness monitoring, and the area of deposited substrate is limited, vacuum-deposition as a mature technique largely eliminates interference factors. Besides, semiconducting film fabricated by this technique is relatively flat and uniform, which facilitates the fundamental mechanism study of OTFTs.[1,22,27] From the research point of view, vacuum-deposition is still a preferable choice in OTFT fabrication. With the progress of molecular design and device fabrication, another kind of film fabrication has attracted more and more attention. Diverse printed[28–30] and solution-processed[15,31–38] methods were invented and utilized for research of low-cost applications.

Different from the perfect structure of single crystals, molecular packing in vacuum-deposited or solution-processed films is influenced by a lot of factors (*e.g.*, vacuum degree, sublimed/evaporated speed, substrate category, roughness, temperature, *etc.*), and a small change of any aspect will result in distinct deposition behavior. Abundant unavoidable defects of semiconducting films make most of OTFTs difficult to reveal the intrinsic properties of semiconductors, which single crystal field-effect transistors (SCFETs) could easily realize.[39–43] Therefore, researchers of OTFTs spent considerable effort on the relationships of temperature, vacuum, morphology, and film thickness with the electrical properties, expecting to improve device performance by optimal combination of device components. Recently, some charming techniques of fabricating crystalline films from solution were invented, and the OTFTs based on them showed great improvement of mobility when compared to their vacuum-deposited counterparts.[44,45]

During the past few decades, more and more organic semiconductors were reported to reach or exceed the mobility of amorphous silicon. To forward the practical application of OTFTs, nowadays researchers focus not only on the development of transfer characteristics and convenient fabrication techniques, but also on the improvement of device stabilities.[46–51] A mobility of 1 $cm^2 V^{-1} s^{-1}$ is taken as watershed in this review, we summarize the SMWCs which exhibit field-effect mobility higher than it, followed with the particular device structure and tested conditions.

P-type semiconductors

Pentacene (**1**),[52] possessing a HOMO energy level of −5.14 eV and a narrow E_g of 1.77 eV, is one of the most popular acenes used as a p-type semiconductor.[53] It is well known that pentacene is fragile to oxygen and light. Especially when pentacene is dissolved, the color of the solution bleaches pretty quickly when exposed to air and light.[54–58] Though the photooxidation tests of evaporated films of pentacene by X-ray photoelectron spectroscopy showed that the oxidation did not obviously speed up under irradiation, there were some oxygen-containing species that coexisted in the surface of the pentacene-based films.[59] Infrared absorption measurements carried out by Palstra *et al.* has showed that 6,13-pentacenequinone (PQ, Scheme 1) is the dominant impurity of commercially available pentacene.[60] Tolbert *et al.* proved that beside PQ, there are other impurities formed during sublimation, including 6,13-dihydropentacene (DHP, Scheme 1) and peripentacene(PP)-containing disproportionation byproducts thus induced.[57]

However, various optimization around pentacene-based OTFTs were carried out due to the intrinsic high performance of pentacene.[60] A high mobility of pentacene-based OTFT which

Wenping Hu

Wenping Hu is a Professor at the Institute of Chemistry, Chinese Academy of Sciences. He received his Ph.D from the Institute in 1999. Then he joined Osaka University, Stuttgart University as a research fellow of Japan Society for the Promotion of Sciences and Alexander von Humboldt, respectively. In 2003 he worked in Nippon Telephone and Telegraph, and then returned to the institute. He focuses on molecular electronics and has more than 180 refereed publications with citations over 2000.

Daoben Zhu

Daoben Zhu is a professor at the Institute of Chemistry, Chinese Academy of Sciences. He was selected as an academician of Chinese Academy of Sciences in 1997. He graduated in 1968 from East China University of Science and Technology. As a visiting scientist he performed research with Prof. Heiz Staab in the Max-Planck Institute for Medical Research in Heidelberg during 1977–1979 and 1985–1986. He served as a vice-director (1988–1992), and director (1992–2000) of the Institute of Chemistry and vice-president of the National Natural Science Foundation of China (2000–2008). His research interests include molecular materials and devices.

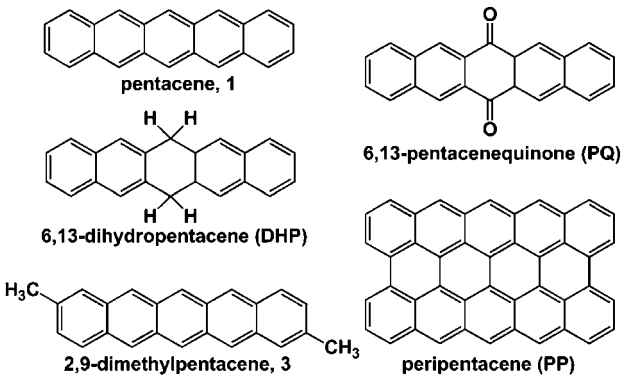

Scheme 1 Chemical structures of pentacene (**1**), 6,13-pentacenequinone (PQ), 6,13-dihydropentacene (DHP), peripentacene (PP) and 2,9-dimethylpentacene (**3**).

was reported by Kelley and co-workers reached as high as 5.0 $cm^2 V^{-1} s^{-1}$ (Fig. 1).[61] The key point in device fabrication was modifying the dielectric with self-assembled monolayers (SAMs) of poly(α-methylstyrene), which was different from the phosphonic acid-based SAMs they used in previous work.[62] A high-ordered film with large grains formed on the homopolymer-modified interface during deposition of pentacene. The authors believed that the smooth polymeric layer made the dielectric surface energy match to pentacene better.[63] Therefore, the main reason for the high performance was attributed to improved growth of the first molecular layer, benefiting from the friendly polymeric substrate. Recently, a very high mobility (23.2 $cm^2 V^{-1} s^{-1}$) of solution-processed pentacene-based OTFT was reported by Hwang *et al.*[64] During the fabrication of the device, a flexible poly(ethylene terephthalate) (PET) substrate was patterned with Au as gate electrodes, then a gate dielectric of a 30 nm thick silk fibroin was fabricated by a three-step process (spin coating, dipping and heating) (Fig. 1). The roughness of this dielectric layer was *ca.* 0.3 nm, which was important for the following vacuum deposition of pentacene.

Picene (**2**) is an isomer of pentacene. It is interesting to note that picene possesses a much larger energy gap (3.3 eV) and a larger ionization potential (5.5 eV) than those of pentacene, which makes picene much more chemically stable. The first OTFT based on picene was reported by Okamoto and co-workers (Fig. 2).[65] They fabricated OTFTs by thermally evaporating picene onto the hexamethyldisilazane-treated SiO_2/Si substrates. Transfer curves were recorded in both forward and reverse modes. Device mobilities increased prominently after exposure to air for a long time or exposure to O_2 for a few hours, and the highest device mobility of 1.75 $cm^2 V^{-1} s^{-1}$ was observed after exposure to O_2 for 70 h. Besides, on/off current ratios of devices were also observed to increase at the same condition. This remarkable increase in both μ_{FET} and the on/off ratio indicated that air (or O_2) took part in channel transport of picene OTFTs, which implied potential application of these devices toward O_2 sensors.

In order to discover promising organic semiconductors, considerable research around pentacene derivatives were carried out. Synthesists tried to adjust molecular properties by introducing different functional groups into the pentacene framework. Kelley and co-workers utilized alkylphosphonic acid, which had a strong affinity for alumina surfaces, to modify the substrates with spin-coated monolayers.[62] A polycrystalline film of 2,9-dimethylpentacene (**3**, Scheme 1) could easily grow on this smooth, passivated surface. A remarkable mobility of 2.5 $cm^2 V^{-1} s^{-1}$ was observed in 2,9-dimethylpentacene-based OTFTs.

Though pentacene derivatives exhibited outstanding performance in the domain of OTFTs, their disadvantages, such as complicated synthesis, difficult purification and low stability, pushed reseachers to find substituents. Eliminating the oxidation possibility by changing the most reactive groups or by introducing substituents into reactive positions is an effective way to design stable molecules.

Take anthradithiophene[55,66] as core, Anthony and co-workers placed trialkylsilylethynyls on the central aromatic ring to form a series of highly soluble derivatives, among which 5,11-bis((triethylsilyl)ethynyl)anthra[2,3-*b*:6,7-*b*′]dithiophene (**4**) adopted a prominent 2-D π-stacking arrangement with π-face separation as small as 3.25 Å in solid states (Fig. 3).[67] The researchers adopted bottom-contact configuration and modified gold electrodes with pentafluorobenzenethiol to improve the gold surface. With the help of a plastic blade, 1–2 wt% solution of **4** in toluene was spread across the device surface, followed by annealing at 90 °C in air. Remarkably, OTFTs based on these uniform films of **4** yielded hole mobility up to 1.0 $cm^2 V^{-1} s^{-1}$ with an on/off current ratio of 10^7. The authors attributed the high performance to the excellent quality of films and close π-stacked interactions in solid states.

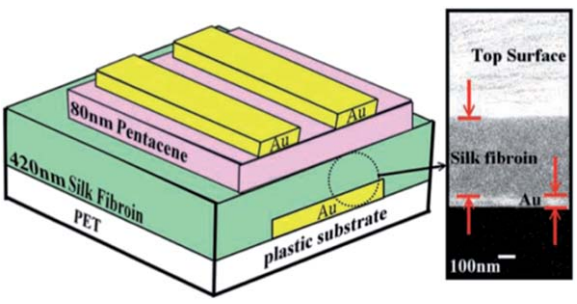

Fig. 1 Schematic (left) and cross-sectional field emission scanning electron microscopy (FESEM) image (right) of pentacene-based OTFT with silk fibroin as the gate dielectric. Reproduced with permission from ref. 64. Copyright 2011 Wiley-VCH Verlag GmbH & Co. KGaA.

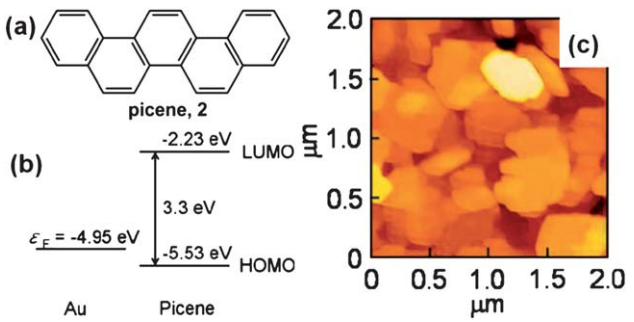

Fig. 2 (a) Molecular structure of picene (**2**); (b) energy diagram of picene; (c) AFM image of picene-based film. Reproduced with permission from ref. 65. Copyright 2008 American Chemical Society.

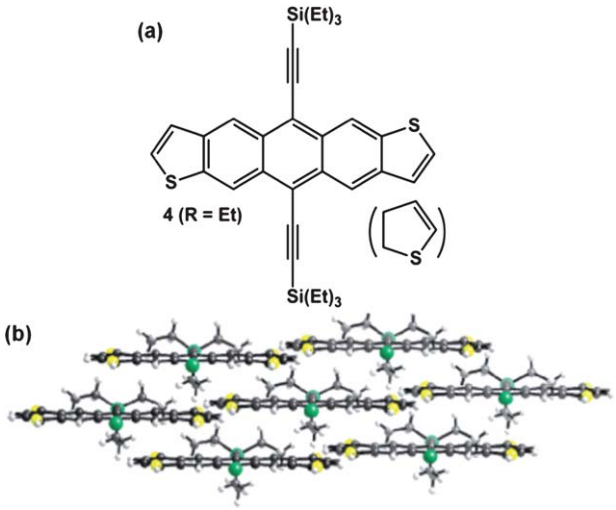

Fig. 3 (a) Chemical structure and (b) crystalline order of **4**. Reproduced with permission from ref. 67. Copyright 2005 American Chemical Society.

Hydrogen-bonds were generally accepted as an effective way to control the intermolecular interactions in organic films.[68,69] Anthony and co-workers partially fluorinated the hetero-aromatic core of **4** to afford ((2,8-difluoroanthra[2,3-*b*:6,7-*b*′] dithiophene-5,11-diyl)bis(ethyne-2,1-diyl))bis(triethylsilane) (**5**, Fig. 4),[70] expecting to accelerate the molecular crystallization and to improve the molecular thermal- and photo-stability by introduction of fluorine-based interactions.[71–74] More significantly, the addition of F···F and F···S interactions improved the molecular packing and resulted in two-dimensional film growth. With an electrode treated by pentafluorothiophenol, OTFTs fabricated on uniform spin-cast films of **5** exhibited the highest performance up to 1.5 $cm^2\ V^{-1}\ s^{-1}$.

Bao and co-workers synthesized a series of asymmetric tetraceno[2,3-*b*]thiophene derivatives, among which 5,12-bis(tri-isopropylsilylethynyl)tetraceno[2,3-*b*]thiophene (TIPSEthiotet, **6**, Fig. 5) showed the most promising 2-D π-stacking in the crystal structure.[75] TIPSEthiotet was vacuum deposited onto bare and OTS-treated SiO_2/Si substrates, followed by research into the substrate temperature–morphology relationship. High quality films in which brick layers oriented parallel to the substrate planes were obtained on the SiO_2/Si substrate at 60 °C. Top-contact OTFTs fabricated in this condition yielded the highest mobility up to 1.25 $cm^2\ V^{-1}\ s^{-1}$.

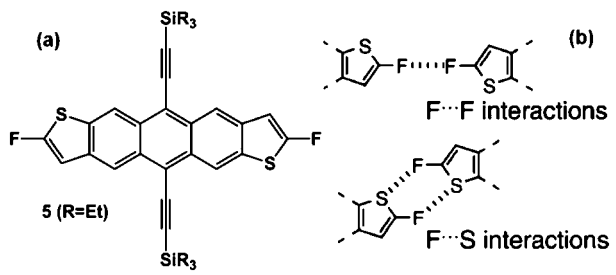

Fig. 4 (a) Chemical structure of **5**; (b) expected F···F and F···S interactions. Reproduced with permission from ref. 70. Copyright 2008 American Chemical Society.

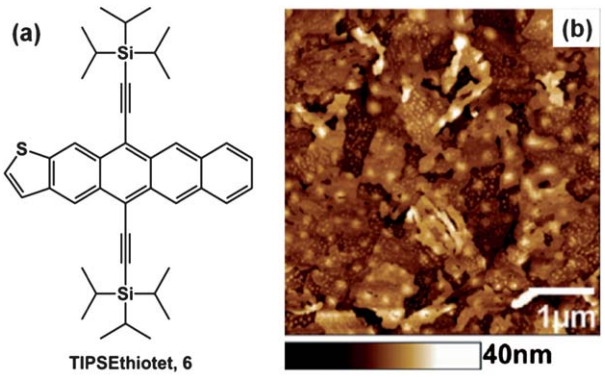

Fig. 5 (a) Chemical structure of TIPSEthiotet (**6**); (b) AFM image of a **6**-based film deposited at 60 °C. Reproduced with permission from ref. 75. Copyright 2008 American Chemical Society.

Replacing benzene with heteroaromatic groups is another strategy to improve molecular oxidation stability. As more and more fused chalcogenophene compounds were proved to be high-performance organic semiconductors, a lot of heteroacenes containing single or unsaturated bonds were designed and synthesized.[76–82] Lowering the HOMO energy level at the same time enlarging E_g was a trait when thiophene or selenophene was introduced into acenes.[83] Takimiya and co-workers utilized the Suzuki–Miyaura coupling reaction to synthesize air-stable 2,7-diphenyl[1] benzothieno[3,2-*b*][1]benzothiophene (DPh-BTBT, **7**, Fig. 6).[46] The HOMO energy level estimated from the oxidation onset was as low as −5.60 eV, and the HOMO–LUMO energy gap calculated from the onset absorption of DPh-BTBT in dilute solution was up to 3.2 eV. SiO_2/Si substrates were subjected to three types of treatment: bare, octyltrichloro silane (OTS) and hexamethyldisilazane (HMDS). Thin films that were vacuum deposited on these substrates were investigated by X-ray diffraction, and the calculated *d*-spacing was proof that DPh-BTBT adopted a nearly perpendicular orientation to the substrates in films. Different from the performance of bare SiO_2/Si-based devices, the mobilities of top-contact OTFTs based on

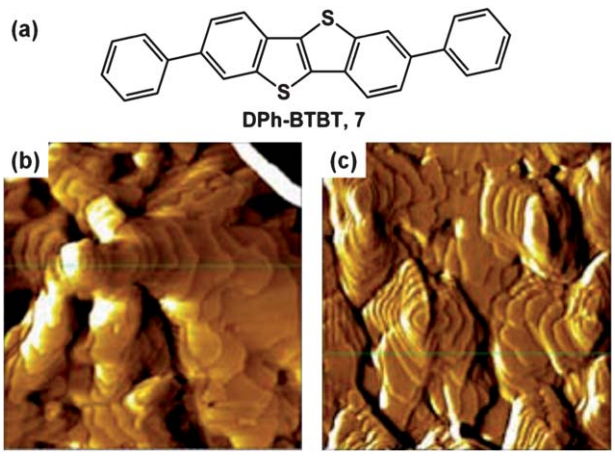

Fig. 6 (a) Chemical structure of DPh-BTBT (**7**); AFM images (4 μm × 4 μm) of **7**-based films deposited on (b) HMDS-treated and (c) OTS-treated SiO_2/Si substrates at T_{sub} = 100 °C. Reproduced with permission from ref. 46. Copyright 2006 American Chemical Society.

silanized substrates showed great dependence on T_{sub}. The maximum μ_{FET} on HMDS-treated and OTS-treated substrates were 1.2 $cm^2\ V^{-1}\ s^{-1}$ and 2.0 $cm^2\ V^{-1}\ s^{-1}$ at T_{sub} = 100 °C, respectively. High stability of the device was proved by the shelf lifetime test over 250 days.

Takimiya *et al.* designed a series of soluble semiconductors[84] based on [1]benzothieno[3,2-*b*][1] benzothiophene (BTBT), which had been proved as a promising core structure for air-stable organic semiconductors. Two long alkyl groups (C_nH_{2n+1}, n = 5–14) were introduced in the long-axis direction of BTBT to facilitate lateral intermolecular interaction. Thus the obtained C_n-BTBT (Fig. 7) were quite soluble in common organic solvents. The active layers used in OTFTs were deposited on the SiO_2/Si substrates by spin coating a 0.4 wt% solution of C_n-BTBT in chloroform at 4000 rpm for 30 s, and annealing at 80 °C under nitrogen. After thermal evaporation of gold (80 nm), the top-contact OTFTs were then annealed at 80 °C under nitrogen again. These OTFTs exhibited prominent performance, in which a best mobility of 2.75 $cm^2\ V^{-1}\ s^{-1}$ with an on/off current ratio of 10^7 was obtained by C_{13}-BTBT (**8**). Molecular packing in a single crystal was observed as a layer-by-layer structure consisting of alternately stacked alkyl layers and BTBT core layers. In the core layers, the abundant S···S, S···thiophene and C–H···π short contacts in a Herringbone structure greatly facilitated the 2-D transport property of the carriers. The X-ray diffraction peaks of the films were assigned very well by single-crystal lattice, showing that the structure in the thin film was identical with that in the single crystal. This was considered as the critical reason for high performance. In the following experiments, they found the *c*-axis lengths of the crystallographic unit cells corresponded to inter-layer distances which were calculated by out-of-plane XRD analyses of the thin films, suggesting that C_n-BTBT crystallites oriented themselves with the *c*-axis along the substrate normal and with the *ab* plane in the in-plane direction.[85] What was interesting to note was that the unit cells and S···S distances became smaller as the alkyl chains elongated, implying that a hydrophobic interaction between the alkyl chains effectively enhanced the intermolecular interaction in the BTBT layers. Furthermore, researchers vacuum deposited C_n-BTBT to fabricate top-contact OTFTs, and a very high mobility, up to 3.9 $cm^2\ V^{-1}\ s^{-1}$, was achieved by C_{12}-BTBT (**9**)-based devices on ODTS-modified substrates.

Subsequently, Takimiya *et al.* successfully synthesized highly π-extended dinaphtho[2,3-*b*:2′,3′-*f*]chalcogenopheno [3,2-*b*] chalcogenophene (DNTT, **10** and DNSS, **11**, as shown in Fig. 8) by three steps.[86] Cyclic voltammetry and UV-vis spectra showed that they possessed low HOMO energy levels (DNTT: −5.44 eV, DNSS: −5.38 eV) and large optical energy gaps (DNTT: 3.0 eV, DNSS: 2.9 eV). The X-ray structural analysis showed that the almost planar molecules of DNTT adopted a Herringbone packing mode in the single crystal, which resulted in a two-dimensional molecular network in the solid states. HMDS and OTS were used to modify the dielectric surfaces. Outstanding performance was observed in top-contact vacuum-deposited OTFTs, wherein the highest μ_{FET} of DNTT and DNSS reached 2.9 $cm^2\ V^{-1}\ s^{-1}$ and 1.9 $cm^2\ V^{-1}\ s^{-1}$ on OTS-treated substrates.

Using the same strategy as that used to change BTBT to C_n-BTBT derivatives, a series of C_n-DNTT (n = 6, 8, 10, 12) were synthesized by Takimiya and co-workers.[87] However, the solubility of these compounds were too low to fabricate solution-processed OTFTs. Vacuum-deposited top-contact OTFTs were fabricated on bare, OTS-treated and ODTS-treated SiO_2/Si substrates. Surprisingly, the performance of the devices fabricated on ODTS-treated substrates showed great dependence on channel length. A highest mobility of 7.9 $cm^2\ V^{-1}\ s^{-1}$ was obtained by depositing C_{10}-DNTT (**12**, Fig. 9) on a ODTS-treated

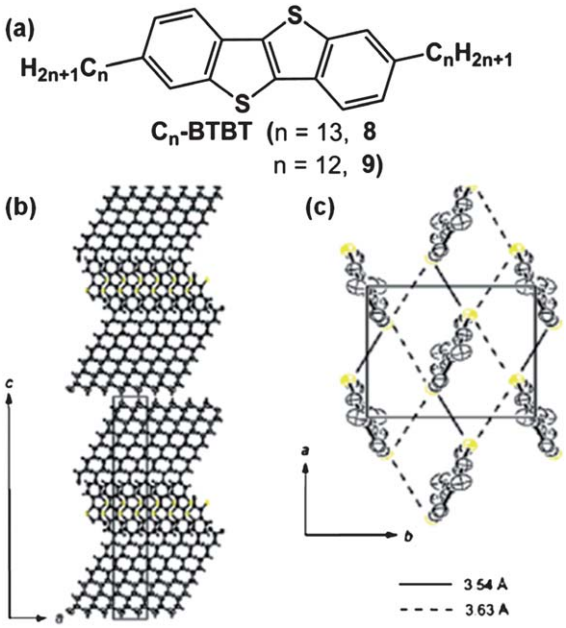

Fig. 7 (a) Molecular structure of C_n-BTBT; (b) crystal structure of C_{12}-BTBT: alternately stacked aliphatic layers and BTBT layers; (c) Herringbone structure in BTBT layer. Reproduced with permission from ref. 84 (Copyright 2007 American Chemical Society).

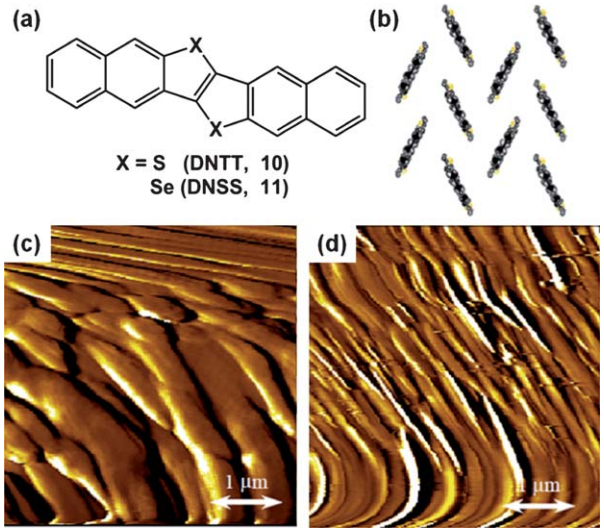

Fig. 8 (a) Chemical structure of DNTT (**10**) and DNSS (**11**); (b) crystal structure of DNTT; (c) film of DNTT deposited on OTS-treated substrate at T_{sub} = 60 °C; (d) film of DNSS deposited on OTS-treated substrate at room temperature. Reproduced with permission from ref. 86. Copyright 2007 American Chemical Society.

substrate with a channel length of 190 μm. The crystalline film of C_{10}-DNTT was formed by gradually shifting droplets of its hot solution with an inclined object on plastic or silicon substrates, followed by dipping into the same solution to fill the cracks. OTFTs based on the films which were formed on SiO_2/Si substrates showed high mobility up to 11 $cm^2\ V^{-1}\ s^{-1}$.[45]

Anthracene, a semiconducting material possessing a relatively large band gap, was utilized as a core to develop an air-stable conjugated system by Meng and co-workers.[47,48] Vinyl, as an important π-electron bridge, was introduced into the backbones of the novel semiconductors, 2,6-bis[2-(4-pentylphenyl)vinyl] anthracene (DPPVAnt, **13**, Fig. 10).[47] The optical band gap of DPPVAnt calculated from the onset wavelength of UV-vis absorption was more than 1 eV wider than that of pentacene. Mobilities of top-contact OTFTs showed great dependence on substrate temperatures, ranging from 0.1 $cm^2\ V^{-1}\ s^{-1}$ to 1.28 $cm^2\ V^{-1}\ s^{-1}$. The best performance device retained a high mobility of 0.95 $cm^2\ V^{-1}\ s^{-1}$ with an on/off current ratio above 10^6 after being stored at ambient conditions for over 20 months. Under similar conditions, ultrapure pentacene exhibited a maximum mobility of 1.05 $cm^2\ V^{-1}\ s^{-1}$, which degraded to ~0.03 $cm^2\ V^{-1}\ s^{-1}$ under ambient conditions in just 1 month. Besides, what was interesting to note was that the packing mode of the DPPVAnt single crystal was also Herringbone, similar to that of pentacene[88] but with a higher packing density, which is desirable in carrier transportation of OTFTs.

As an analogue of DPPVAnt, di(phenylvinyl)anthracene (DPVAnt, **14**, Fig. 11) was also compared with pentacene in terms of physicochemical and electrical properties.[48] Cyclic voltammetry indicated that the HOMO energy level of DPVAnt was −5.40 eV, as compared to that of pentacene which was −5.00 eV. Optical band gaps estimated from UV-vis absorption spectra were 2.6 eV for DPVAnt and 1.8 eV for pentacene. All these results indicated that DPVAnt possesses superior oxidation stability over pentacene. DPVAnt and pentacene were vacuum deposited onto OTS-modified SiO_2/Si substrates with gold as source/drain electrodes. DPVAnt TFT yielded a mobility of 1.3 $cm^2\ V^{-1}\ s^{-1}$ at T_{sub} = 80 °C while pentacene TFT reached a mobility of 1.0 $cm^2\ V^{-1}\ s^{-1}$ at T_{sub} = 60 °C. With respect to device performance (mobility, on/off current ratio, threshold voltage, subthreshold swing, *etc.*), the most striking difference between the two devices was that the $V_{turn\text{-}on}$ and V_{th} of the DPVAnt OTFTs were much more negative than those of pentacene OTFTs. For comparison of device stability, DPVAnt and pentacene were vacuum deposited onto the glass substrates with Al gate electrodes coated by a self-assembled monolayer of phosphonic acid. During cycle and shelf-life tests, pentacene OTFTs displayed a significant degradation in performance, while the mobility of DPVAnt OTFTs were almost unaffected. The

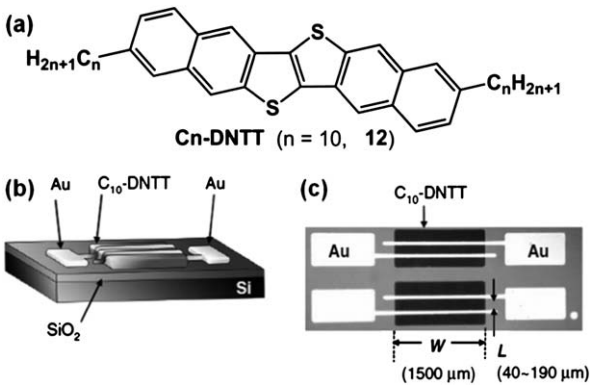

Fig. 9 (a) Molecular structure of C_n-DNTT (n = 6, 8, 10, 12); (b) schematic representation of device structure; (c) top view of OTFTs. Reproduced with permission from ref. 87. Copyright 2011 Wiley-VCH Verlag GmbH & Co. KGaA.

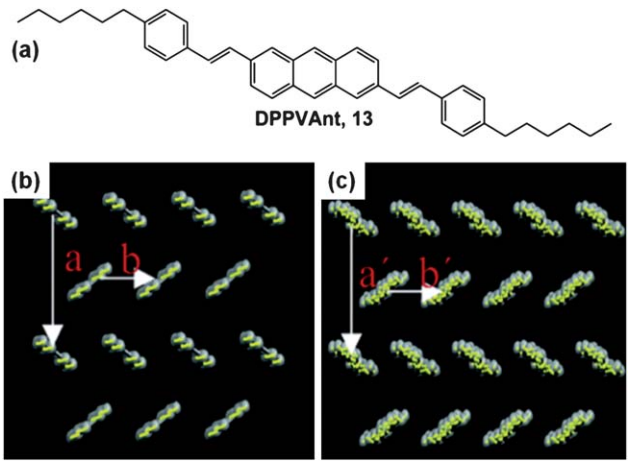

Fig. 10 (a) Molecular structure of DPPVAnt (**13**); molecular packing of (b) pentacene (a = 7.79 Å, b = 6.27 Å) and (c) DPPVAnt (a' = 7.23 Å, b' = 5.85 Å). Reproduced with permission from ref. 47. Copyright 2006 American Chemical Society.

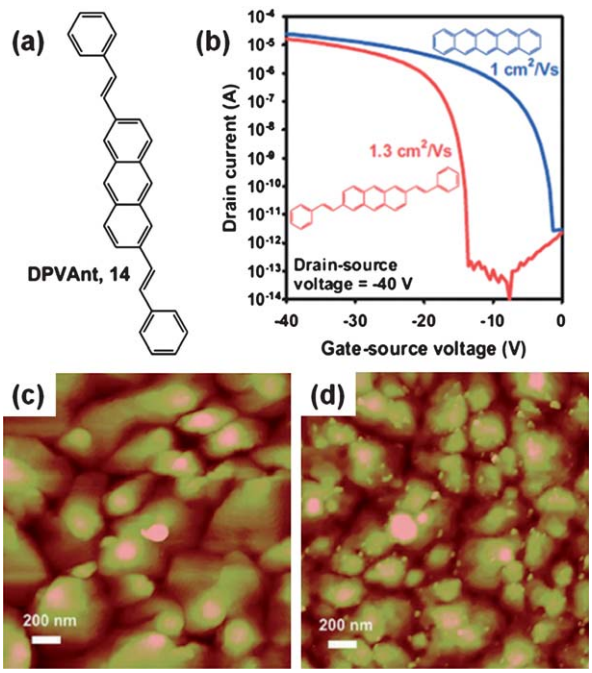

Fig. 11 (a) Molecular structure of DPVAnt (**14**); (b) transfer characteristics of DPVAnt-based OTFTs and pentacene-based OTFTs; AFM images of (c) DPVAnt film and (d) pentacene film deposited on OTS-treated SiO_2/Si substrates. Reproduced with permission from ref. 48. Copyright 2007 Wiley-VCH Verlag GmbH & Co. KGaA.

authors attributed this phenomenon to the more negative HOMO energy level of DPVAnt compared to pentacene. Besides, researchers fabricated five-stage ring oscillators to evaluate the dynamic performance of two transistors. The ring oscillator delay of both semiconductors were very similar.

Wang and co-workers synthesized vinyl containing dimer *trans*-1,2-(dithieno[2,3-*b*:3′,2′-*d*]thiophene)ethene and its derivatives.[49] Compounds with different substituents showed great difference in performance of vacuum-deposited top-contact OTFTs. The most promising compound, terminated by phenyl (**15**, Fig. 12), showed mobilities ranging from 0.28 to 2.0 $cm^2 V^{-1} s^{-1}$, in which the highest mobility was obtained on the basis of a continuous film deposited by a two-stage technique. No obvious change of mobility was found when the device was stored for more than 7 months, indicating excellent stability.

Besides vinyl, ethynyl was another unsaturated bond which possessed much shorter bond length and tighter electronic distribution. A lot of synthesists tried to regulate molecular properties by introducing ethynyl into the molecular long-axis direction.[89–92] Recently, Hu and co-workers designed and synthesized a series of ethynylene-containing benzodithiophene derivatives, and developed the field-effect properties of benzodithiophene by introduction of aryl-acetylenes (Fig. 13).[93] High performance of 0.72 $cm^2 V^{-1} s^{-1}$ with an on/off current ratio of 10^7 was easily obtained when BPEBDT (**16**) was vacuum-deposited on OTS-treated substrates at room temperature, indicating the potential application in flexible devices. A two-step deposition was used to improve the quality of the active layer, and the most continuous terrace film was deposited at 100 °C/50 °C with respective thicknesses of 10 nm/50 nm. Based on this high-quality film, OTFT showed the highest mobility up to 1.17 $cm^2 V^{-1} s^{-1}$. In addition, a vacuum-deposited film of BPEBDT based on quartz was stored at ambient conditions for 12 months. Comparison of UV-vis absorption spectra of the film before and after storage showed nearly no change, indicating the high environmental stability of the compound.

Hexamethylenetetrathiafulvalene (HMTTF, **17**), which had been reported to exhibit a mobility of 11 $cm^2 V^{-1} s^{-1}$ in a single-crystal transistor, was chosen as a parent compound for alkyl

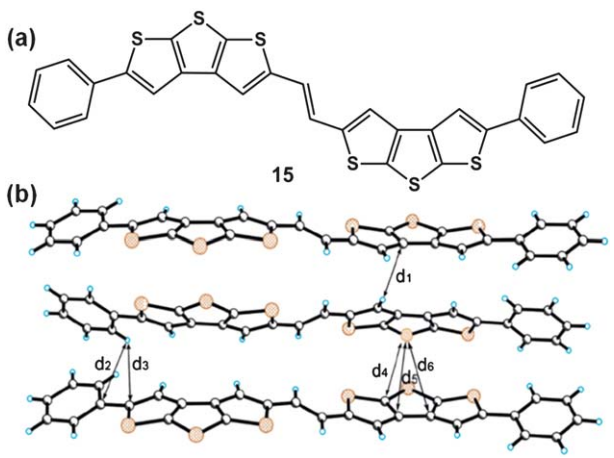

Fig. 12 (a) Molecular structure of **15**; (b) short contacts between neighboring molecules in the crystal structure of **15**. Reproduced with permission from ref. 49. Copyright 2009 American Chemical Society.

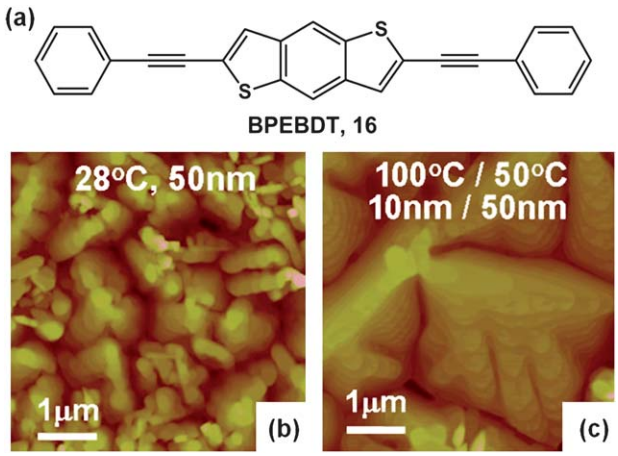

Fig. 13 (a) Chemical structure of BPEBDT (**16**); AFM images of BPEBDT film deposited at (b) room temperature and (c) 100 °C/50 °C. Reproduced with permission from ref. 93. Copyright 2010 The Royal Society of Chemistry.

derivation by Mori and co-workers (Fig. 14).[94] The highest mobility of 3.6 $cm^2 V^{-1} s^{-1}$ still belonged to the HMTTF-based OTFT but with a low on/off current ratio of 10^3 and relatively large positive V_{th} of 27 V. However, the compound substituted by *tert*-butyl (**18**) exhibited high mobilities of ~1 $cm^2 V^{-1} s^{-1}$ in the top-contact OTFT, which was fabricated by vacuum depositing semiconductors on a OTS-treated SiO_2/Si substrate at T_{sub} = 50 °C. The high mobility and low threshold voltage were maintained for more than one month in air. The authors believed that it was the passivation layer formed by closely packed alkyl groups that greatly stabilized the device performance.

Titanyl phthalocyanine (TiOPc, **19**) was an efficient organic photoconductor that was used as non-toxic ink powder.[95] Different from other phthalocyanines, TiOPc was a polar molecule with titanyl perpendicular to the nearly planar macrocycle (Fig. 15). The triclinic α-structure (α-phase TiOPc) was

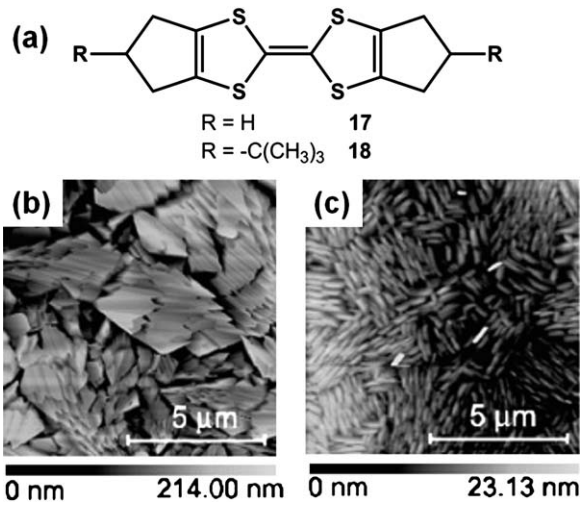

Fig. 14 (a) Molecular structure of HMTTF (**17**) and *tert*-butyl substituted HMTTF (**18**); AFM images of films deposited by (b) **17** and (c) **18**. Reproduced with permission from ref. 94. Copyright 2009 The Royal Society of Chemistry.

one of the three crystal structures of TiOPc reported thus far, and the TiOPc molecules could form surprisingly rigid packing of concave and convex pairs only in this phase. Hu *et al.* successfully obtained films of pure α-TiOPc by vacuum depositing TiOPc onto OTS-modified SiO_2/Si substrates at $T_{sub} \geq 120$ °C, in which TiOPc molecules preferentially stood on the substrates with an "edge-on" style orientation.[50] UV-NIR spectra and XRD analysis confirmed the results. Top-contact OTFTs were fabricated on the basis of an α-phase film at 150 °C, and the best performance of 161 selected devices reached 10 $cm^2 V^{-1} s^{-1}$. The authors attributed this extraordinary performance to the ultra close π-stack of α-TiOPc molecules in favorable "edge-on" orientation. Distribution of device performance showed that over 90% of the devices exhibited a μ_{FET} above 1 $cm^2 V^{-1} s^{-1}$, and over 97% of the devices exhibited an on/off current ratio above 10^6. During the stability test over 180 days, only a ~20% decrease was observed in the first few days, followed by stable performance for a long time. Calculated results showed that the strongest electronic coupling of TiOPc and pentacene was 0.143 eV and 0.093 eV, whereas the calculated hole reorganization energy of TiOPc and pentacene was 0.079 eV and 0.095 eV, respectively. All the results showed TiOPc was a promising candidate for OTFTs.

Non-planar vanadyl phthalocyanine (VOPc, **20**, Fig. 16) has a similar molecular structure as TiOPc. Yan *et al.* utilized para-sexiphenyl (*p*-6P) to modify sputtered Al_2O_3/Si substrates, followed by vacuum-deposition of VOPc at 180 °C.[96] The atomic force microscopic (AFM) analysis showed these films consisted of intimately connected lamellar crystals. X-ray diffraction spectrum indicated that the VOPc molecules were standing up on the *p*-6P film. Top-contact OTFTs of VOPc exhibited the highest mobility of 1.23 $cm^2 V^{-1} s^{-1}$.

Driven by application of low-cost large-scale flexible electronics, various solution-processed techniques were invented for deposition of semiconducting films, in which a few techniques based on particular compounds showed well-ordered film and high mobilities.[44,45,97] A zone-casting solution-processed technique invented by Müllen *et al.* afforded well-arranged films of HBC-C_{12} (**21**, Fig 17),[97] which possessed a high intrinsic mobility up to 1.1 $cm^2 V^{-1} s^{-1}$. By using this technique, the OTFTs based on long-range-oriented films of **21** exhibited the highest mobility only up to 1×10^{-2} $cm^2 V^{-1} s^{-1}$, which should be attributed to the substantial boundaries among ribbons. Therefore, technique inventions of large-area crystalline film are desirable.

Very recently, a solution-casting technique to fabricate millimeter-sized single-crystal films was invented by Hu *et al.*[44] Chlorobenzene solutions of HTEB (**22**, Fig. 18) were cast onto Si, SiO_2, quartz and other non-crystalline substrates, then the compound self-assembled on the substrates at room temperature for at least 24 h. These rapidly assembled films, whose size reached as large as the millimeter scale, showed no dependence on substrate categories. The roughness of these films obtained by atomic force microscopy (AFM) was only 0.3–0.4 nm. Selected area electron diffraction (SAED) patterns of different parts of the same film are unique, indicating the whole film was a single crystal. OTFTs based on these high-quality films exhibited mobilities up to 1.0 $cm^2 V^{-1} s^{-1}$, which was 10 times higher than that of vacuum-deposited devices.[90]

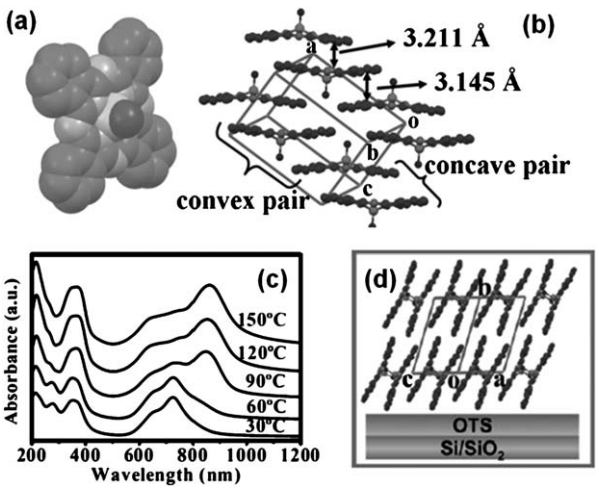

Fig. 15 (a) Space-filling molecular model of TiOPc (**19**); (b) molecular stacking of α-TiOPc in single crystal; (c) UV-NIR absorption spectra of TiOPc films on OTS-modified substrate at different substrate temperatures; (d) the "edge-on" style of molecular orientation in α-TiOPc. Reproduced with permission from ref. 50. Copyright 2007 Wiley-VCH Verlag GmbH & Co. KGaA.

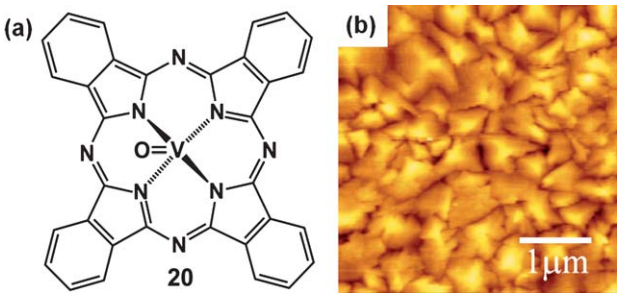

Fig. 16 (a) Molecular structure of VOPc (**20**); (b) AFM image of film consisted of VOPc (30 nm)/*p*-6P (3 nm). Reproduced with permission from ref. 96. Copyright 2007 American Institute of Physics.

N-type semiconductors

Compared to abundant high-performance p-type semiconductors, n-type semiconductors have not fully developed. A lot of synthesized n-type semiconductors could not meet the

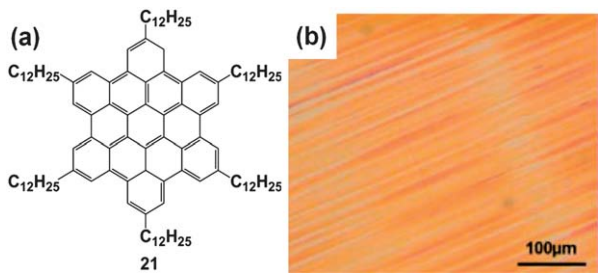

Fig. 17 (a) Molecular structure of HBC-C_{12} (**21**); (b) optical microscopy image of a zone-cast **21**-based film on a silicon substrate. Reproduced with permission from ref. 97. Copyright 2005 Wiley-VCH Verlag GmbH & Co. KGaA.

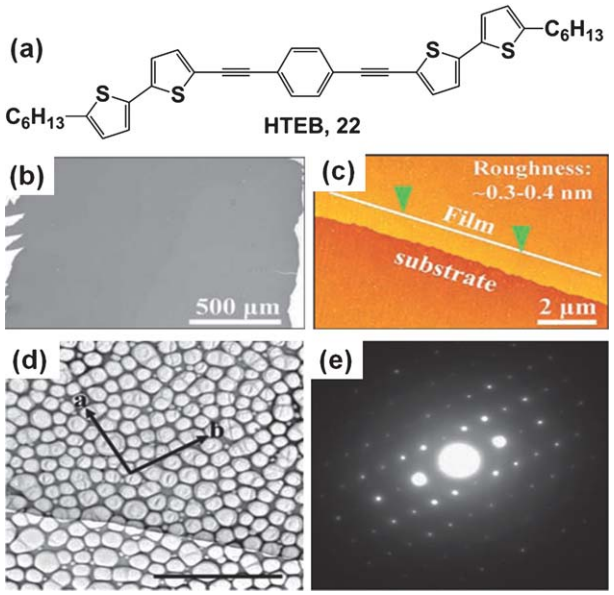

Fig. 18 (a) Molecular structure of HTEB (**22**); (b) SEM image, (c) AFM image, (d) TEM image (the scale bar is 10 μm) and (e) SAED pattern of cast-assembled HTEB-based films. Reproduced with permission from ref. 44. Copyright 2011 Wiley-VCH Verlag GmbH & Co. KGaA.

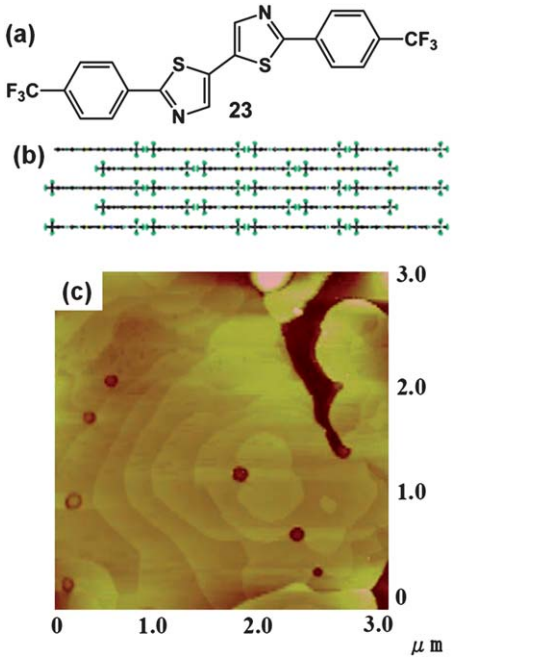

Fig. 19 (a) Molecular structure of 2,2′-bis(4-(trifluoromethyl)phenyl)-5,5′-bithiazole (**23**); (b) stacking structure of **23** along the *c*-axis in single crystal; (c) AFM image of film of **23** deposited on OTS-treated substrate at 25 °C. Reproduced with permission from ref. 98. Copyright 2005 American Chemical Society.

expectation of the designers, even with no field-effect performance in air. One reason for this is the instability of organic anions under ambient conditions where oxygen and water are sufficient. Therefore, many n-type transistors can only be fabricated and tested under inert conditions to avoid the influence of oxygen and water. Another reason for poor performance is the injection barrier between the LUMO level of n-type semiconductors and work function of air-stabled electrodes (*e.g.* Au) normally used in OTFT fabrications.[22]

With the hope to synthesize air-stabled n-channel semiconductors, a series of strong electron withdrawing groups (*e.g.* fluorine, cyano, carbonyl or diimide moieties) were introduced to molecular backbones to increase electron affinities. Theoretically, both the molecular stability and device stability could be improved in this way. Yamashita *et al.* synthesized a series of oligomers containing electron-accepting thiazoles as core system and trifluoromethylphenyl groups as end substituents.[98] Among all compounds 2,2′-bis(4-(trifluoromethyl)phenyl)-5,5′-bithiazole (**23**, Fig. 19) had a completely planar geometry, forming a unique 2-D columnar structure. Its reduction potential measured by differential pulse voltammetry was −1.63 V, and the HOMO–LUMO band gap estimated from absorption onset was 2.90 eV. Top-contact OTFTs were fabricated by vacuum depositing **23** onto bare, HMDS-treated and OTS-treated substrates, followed by thermal evaporation of gold as source/drain electrodes. In vacuum, the field-effect mobilities showed great dependence on the modified surface. X-ray diffraction of the films showed sharp reflections up to the second order, indicating formation of lamellar ordering and crystallinity. The highest mobility up to 1.83 $cm^2 V^{-1} s^{-1}$ with V_{th} of 78 V was obtained on OTS-treated SiO_2/Si substrate in a vacuum chamber.

With the same trifluoromethylphenyl end groups, Yamashita *et al.* synthesized 2,5-bis(5-(4-(trifluoromethyl) phenyl)thiophen-2-yl)-3a,6a-dihydrothiazolo[5,4-*d*]thiazole (**24**, Fig. 20).[99] For improving the surface of dielectric, a series of n-alkyl (BTS: butyl-trichlorosilane, OTS: octyl-trichlorosilane, TDTS: tetradecyl-trichlorosilane, and ODTS: octadecyl-trichlorosilane) were employed to form self-assembled monolayers (SAMs) by immersing substrate in the anhydrous solution of silane-coupling agents in toluene for 6 h. Without exposure to air, the modified substrates were subjected to thermal vaporation of **24** and source/drain electrodes (Au) successively, followed by device tests in vacuum. The researchers found that a longer alkyl chain significantly improved the field-effect performance, and the

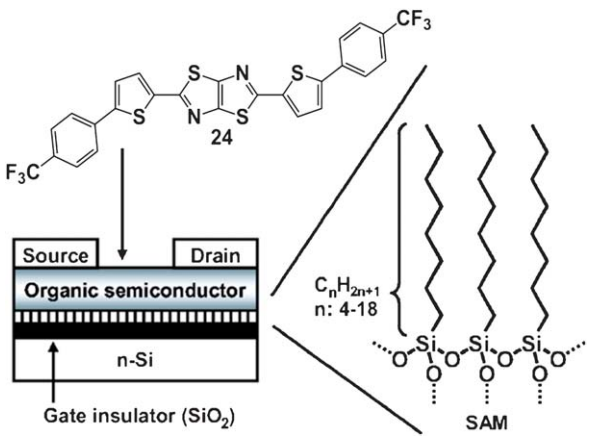

Fig. 20 Chemical structure of **24** and schematic diagram of OTFT structure with self-assembled monolayers. Reproduced with permission from ref. 99. Copyright 2007 American Institute of Physics.

highest electron mobility based on ODTS-treated substrate reached 1.2 $cm^2 V^{-1} s^{-1}$ with an on/off ratio of 10^7. The authors attributed this to the suppression of influence of electron traps on SiO_2 insulator by employing SAM with long alkyl chains.

Shukla *et al.* introduced cyclohexyl, a group that exhibited great conformational rigidity and existed almost exclusively in a chair form, into naphthalene diimides (NDI), with the hope of improving molecular crystalline packing and thin film morphology (**25**, Fig. 21).[100] XRD analysis of the single crystal showed the naphthalene diimide cores were not cofacial along the stacking direction but were displaced along both the short and the long axes of the molecules. The X-ray diffraction of a **25**-based film showed strong and narrow peaks up to the fifth order, indicating the molecular packing motif in the thin film was the same as that in the bulk crystals. Top-contact OTFTs were fabricated by vacuum depositing semiconductor on the OTS-treated substrates, followed by thermal evaporation of gold through a shadow mask. The electrical performance was measured under a continuous stream of argon or oxygen with different humidity. Hysteresis was observed in a double I_D–V_G sweep at constant V_{DS}. The best performance of 7.5 $cm^2 V^{-1} s^{-1}$ was obtained when the device was tested after prolonged equilibration in an argon atmosphere at low humidity.

Perylene diimides (PDIs), a group of organic semiconductors possessing relatively high electron affinity, were extensively used in synthesis of n-channel semiconductors since the π-orbital interactions in solid states could be tuned by changing the substituents on the imide N atoms. Frisbie *et al.* reported the structural and electrical transport properties of a π-stacking soluble n-type semiconductor, *N*,*N*′-dioctyl-3,4,9,10-perylene tetracarboxylic diimides (PTCDI-C8, **26**, Fig. 22).[101] Hydrophilic SiO_2 (yielded by exposing untreated SiO_2 to oxygen plasma or ozone after cleaning) and hydrophobic SiO_2 (formed by spin-coating a thin layer of poly(α-methylstyrene) onto hydrophilic SiO_2) substrates were subjected to thermal evaporation of PTCDI-C8 under vacuum. No observable morphology, grain size or packing difference of films were observed on SiO_2 or PS-SiO_2 substrates. The sharp primary peak of XRD analysis of films corresponded to the first powder pattern (001) peak. The authors proposed that the long axis of the perylene diimide core

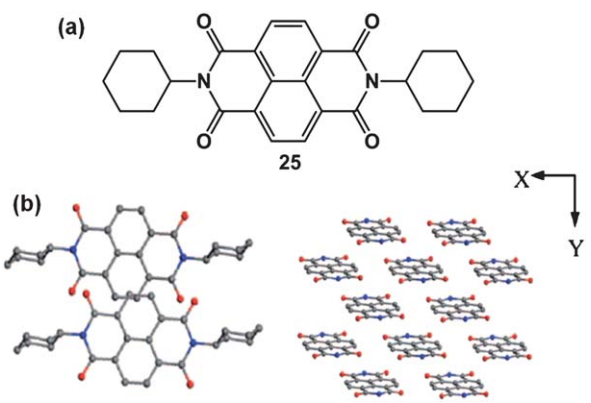

Fig. 21 (a) Molecular structure of *N*,*N*′-bis(cyclohexyl) naphthalene-1,4,5,8- bis(dicarboximide) (**25**); (b) crystal packing of **25**. Reproduced with permission from ref. 100. Copyright 2008 American Chemical Society.

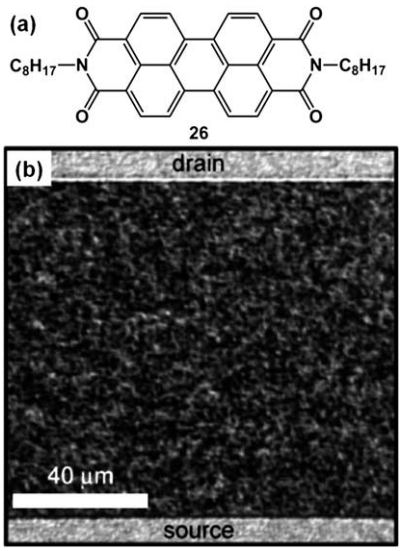

Fig. 22 (a) Molecular structure of PTCDI-C8 (**26**); (b) optical micrograph of **26**-based film (T_{sub} = 75 °C). Reproduced with permission from ref. 101. Copyright 2004 American Chemical Society.

was oriented roughly parallel to the substrate normal, with π-stacking occurring parallel to the substrate surface. Due to this optimal packing scheme of active layer, top-contact OTFTs with Ag as source/drain electrodes reached a mobility as high as 1.7 $cm^2 V^{-1} s^{-1}$ under vacuum or reducing atmospheres.

Ichikawa *et al.* focused on PTCDI derivatives with longer alkyl chain, namely *N*,*N*′-ditridecyl-3,4,9,10-perylene tetracarboxylic diimides (PTCDI-C13, **27**, Fig. 23), with the hope of repairing molecular alignments and crystal disorders by thermal treatment.[102] PTCDI-C13 was thermally evaporated onto the SiO_2 wafer that was thermally grown on heavily doped p-type silicon substrates, followed by thermal evaporation of Au as source/drain electrodes. All TFT characteristics were measured under vacuum (below 5×10^{-4} Pa). After the first measurements of as-prepared OTFTs, the devices were annealed at 140 °C for 1 h and

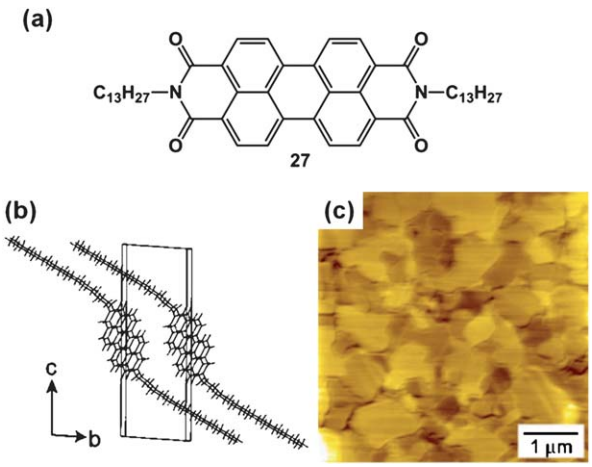

Fig. 23 (a) Chemical structure of PTCDI-C13 (**27**); (b) crystal packing of **27**; (c) AFM image of **27**-based film annealed at 140 °C. Reproduced with permission from ref. 102. Copyright 2006 American Institute of Physics.

then slowly cooled to room temperature under vacuum. The obtained OTFTs exhibited a electron mobility up to 2.1 $cm^2\ V^{-1}\ s^{-1}$ with V_{th} of 60 V under vacuum. Though the devices were exposed to air after thermal treatment, the n-type behavior could only be obtained in vacuum. The sharp reflections of X-ray diffraction up to the fourth order showed up in the thermal-treated films, indicating the crystalline *c*-axis was perpendicularly ordered on the substrate. This result was confirmed by the AFM analyses of annealed active layers.

Fullerene C_{60} and derivatives, which possess exceptionally high electron affinity but poor crystallization, are known as promising n-type semiconductors.[22,103–105] Recently, Itaka *et al.* utilized an atomically flat pentacene monolayer to increase the molecular wettability of the substrate, inducing a better crystallinity of C_{60} (**28**, Fig. 24).[106] For comparison, 20 nm thick C_{60} films were thermally evaporated on the sapphire substrates with and without a 1.5 nm thick pentacene monolayer. AFM analysis of the films showed that the faceted crystalline C_{60} grains with smooth surfaces could be obtained only when pentacene buffer was used. XRD analysis of these films confirmed the C_{60} films with pentacene buffer exhibited strong diffraction peaks of *c**-axis-oriented crystal. With Mg as source/drain electrodes, bottom-gate C_{60} TFTs with pentacene buffer exhibited an ambipolar characteristic, and the highest electron mobility reached 4.9 $cm^2\ V^{-1}\ s^{-1}$, which was 4–5 times higher than that of C_{60} TFT without pentacene buffer. Differently, Anthopoulos *et al.* fabricated OTFTs based on C_{60} films grown by hot wall epitaxy.[107] The electron mobilities showed strong dependence on the substrate temperatures. A very high electron mobility of 6 $cm^2\ V^{-1}\ s^{-1}$ was obtained when the C_{60} film was deposited at T_{sub} = 250 °C. The authors attributed the improvement of mobility to the large grain size of C_{60} formed at elevated substrate temperature. Besides, the use of low work function source/drain (LiF/Al) electrodes also took part in the excellent electron injecting characteristics.

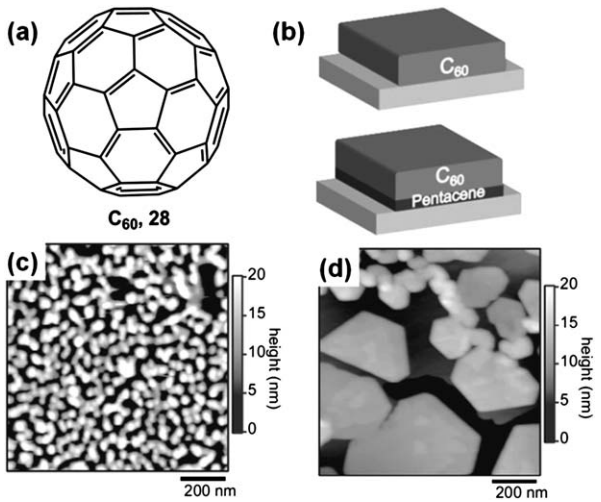

Fig. 24 (a) Structure of C_{60} (**28**); (b) schematic diagram of C_{60} thin film grown on a substrate without (top) and with (bottom) pentacene; (c) AFM image of C_{60} thin film grown on a substrate without pentacene; (d) AFM image of C_{60} thin film grown on a substrate with pentacene monolayer. Reproduced with permission from ref. 106. Copyright 2006 Wiley-VCH Verlag GmbH & Co. KGaA.

A series of silylethynylated *N*-heteropentacene derivatives were designed by Miao *et al.*,[108] in which compound **29** (Fig. 25) showed the shortest π-to-π distance in crystal structures. Based on vacuum-deposited terraced film of **29**, OTFTs showed mobility as high as 3.3 $cm^2\ V^{-1}\ s^{-1}$ under vacuum. Whereas tested in ambient air, the mobility of device decreased to 0.3–0.5 $cm^2\ V^{-1}\ s^{-1}$. Solution processed films were also fabricated, and a mobility of $3 \times 10^{-3}\ cm^2\ V^{-1}s^{-1}$ was obtained by a **29**-based OTFT.

Recently, a naphthalene diimide (NDI) derivative core-expanded by two 2-(1,3-dithiol-2-ylidene)malonitrile moieties (**30**, Scheme 2) was synthesized by Gao *et al.*[109] Estimated by density functional theory (DFT), the LUMO energy level of **30** was 1.1 eV lower than that of NDI, indicating the potential application of air stable OTFTs. After spin-coating on OTS-treated SiO_2/Si substrates, the films of **30** were annealed at different temperatures. The film annealed at 180 °C exhibited electron mobility up to 0.51 $cm^2\ V^{-1}\ s^{-1}$ under ambient conditions. Further they prepared all-solution-processed OTFTs of **30** under ambient conditions, and systematically summarized the performance of devices fabricated with different substrates (silicon, glass, PET), electrodes (Au, modified Au, inkjet-printed Ag), dielectrics(SiO_2, PAN/PMSQ, SiO_2/PAN/PMSQ) and deposition methods (spin-coating, inkjet-printing, brush-painting).[110] When tested in air, the spin-coated active layer on SiO_2/Si with pentafluorobenzene thiol (PFBT)-modified Au electrodes showed electron mobility as high as 1.20 $cm^2\ V^{-1}\ s^{-1}$.

It is easy to note that the introduction of electron withdrawing groups is crucial for n-type semiconductors. Besides, there are some classical core groups whose substitutions are generally promising for n-type organic semiconducting candidates, such as naphthalene diimides (NDIs),[100,111–113] perylene diimides (PDIs),[102,114,115] core-cyanated NDIs,[116] core-cyanated PDIs,[117–119] core-halogenated PDIs,[120,121] *etc.* Notably, OTFTs based on core-cyanated PDIs and NDIs showed high performance and device stability in ambient air, which their cyano-absent counterparts could not reach.

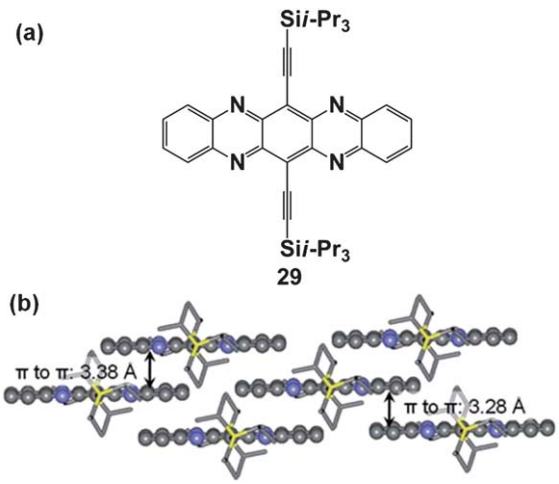

Fig. 25 (a) Molecular structure of compound **29**; (b) crystal structure of **29**. Reproduced with permission from ref. 108. Copyright 2011 Wiley-VCH Verlag GmbH & Co. KGaA.

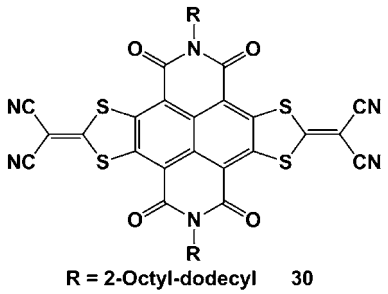

Scheme 2 Molecular structure of compound **30**.

Conclusions

Compared to the optimal packing mode in a single crystal, a thin film of an organic semiconductor derived from vacuum deposition or solution processing is too defective to exhibit the intrinsic transport property of a semiconductor. Therefore, to design molecules that could form compact regular packing in solid states is a general guideline for searching high-performance semiconductors of OTFTs. Among reported high-performance semiconductors, acenes/hetroacenes which possess optimized electronic conjugation and planar structures are popular as parent groups for specific derivation, depending on the requirement of expected molecular physicochemical properties and/or deposition conditions.

Recently, some surprisingly high mobilities have been observed in solution-processed OTFTs, indicating high quality semiconducting films that have good crystallinity and few grain boundaries are required for high-performance OTFTs. Besides, the condition of the dielectric/semiconductor intersurface is critical for deposition of active layers. Totally different deposition behaviors of the same compound are generally observed on the substrates with different modification. During the modification, not only is the surface energy of the dielectric changed, but also the packing mode of the semiconductors. Empirically, treating the substrate with some functional agents (silane-coupling agents, polymers or well-aligned SMWCs) induced better growth of the primary semiconducting monolayers, resulting in high quality semiconducting films.

Nowadays, the lack of air-stable high-performance n-type semiconductors is the most urgent issue in the development of organic semiconductors. Up till now, the amount of high-performance n-type semiconductors is far less than that of p-type semiconductors. Although some high performance n-channel OTFTs have been reported, most of them showed high sensitivity to surrounding conditions (atmosphere, atmospheric pressure, humidity *etc.*) and degraded greatly as soon as they were exposed to air. Besides, the threshold voltages of reported high-performance n-channel OTFTs were relatively high even when they were tested under an inert atmosphere.

For the practical application of OTFTs, more efforts need to be made on 1) inventing an effective way for large-scale solution-processible deposition of semiconductors, 2) improving the n-channel stability against the environment, 3) decreasing the power consumption of device operation. Though there are still many challenges in the field of OTFTs, the widespread use of practical OTFT products can be anticipated in the near future.

Acknowledgements

The authors acknowledged the financial support from National Natural Science Foundation of China (20721061, 20872146, 50725311, 51033006, 51003107), the Ministry of Science and Technology of China (2010CB808400, 2011CB932300) and Chinese Academy of Sciences.

Notes and references

1 A. R. Murphy and J. M. J. Fréchet, *Chem. Rev.*, 2007, **107**, 1066–1096.
2 M. Muccini, *Nat. Mater.*, 2006, **5**, 605–613.
3 W. Wu, Y. Liu and D. Zhu, *Chem. Soc. Rev.*, 2010, **39**, 1489.
4 C. D. Dimitrakopoulos and P. R. L. Malenfant, *Adv. Mater.*, 2002, **14**, 99–117.
5 C. Reese, M. Roberts, M.-m. Ling and Z. Bao, *Mater. Today*, 2004, **7**, 20–27.
6 J. E. Anthony, *Chem. Rev.*, 2006, **106**, 5028–5048.
7 H. E. Katz, Z. Bao and S. L. Gilat, *Acc. Chem. Res.*, 2001, **34**, 359–369.
8 R. A. Pascal, *Chem. Rev.*, 2006, **106**, 4809–4819.
9 M. Bendikov, F. Wudl and D. F. Perepichka, *Chem. Rev.*, 2004, **104**, 4891–4946.
10 A. Dodabalapur, *Mater. Today*, 2006, **9**, 24–30.
11 A. Facchetti, *Mater. Today*, 2007, **10**, 28–37.
12 Y. Li, S. P. Singh and P. Sonar, *Adv. Mater.*, 2010, **22**, 4862–4866.
13 I. Osaka, T. Abe, S. Shinamura, E. Miyazaki and K. Takimiya, *J. Am. Chem. Soc.*, 2010, **132**, 5000–5001.
14 I. McCulloch, M. Heeney, C. Bailey, K. Genevicius, I. Macdonald, M. Shkunov, D. Sparrowe, S. Tierney, R. Wagner, W. M. Zhang, M. L. Chabinyc, R. J. Kline, M. D. McGehee and M. F. Toney, *Nat. Mater.*, 2006, **5**, 328–333.
15 H. N. Tsao, D. Cho, J. W. Andreasen, A. Rouhanipour, D. W. Breiby, W. Pisula and K. Mullen, *Adv. Mater.*, 2009, **21**, 209–212.
16 S. Allard, M. Forster, B. Souharce, H. Thiem and U. Scherf, *Angew. Chem., Int. Ed.*, 2008, **47**, 4070–4098.
17 C. Haensch, S. Hoeppener and U. S. Schubert, *Chem. Soc. Rev.*, 2010, **39**, 2323–2334.
18 Y. Wu, Y. Li, P. Liu, S. Gardner and B. S. Ong, *Chem. Mater.*, 2006, **18**, 4627–4632.
19 Y. D. Park, J. A. Lim, H. S. Lee and K. Cho, *Mater. Today*, 2007, **10**, 46–54.
20 C. A. Di, Y. Q. Liu, G. Yu and D. B. Zhu, *Acc. Chem. Res.*, 2009, **42**, 1573–1583.
21 J. Veres, S. Ogier, G. Lloyd and D. de Leeuw, *Chem. Mater.*, 2004, **16**, 4543–4555.
22 J. Zaumseil and H. Sirringhaus, *Chem. Rev.*, 2007, **107**, 1296–1323.
23 R. Ruiz, A. Papadimitratos, A. C. Mayer and G. G. Malliaras, *Adv. Mater.*, 2005, **17**, 1795–1798.
24 A. Dodabalapur, L. Torsi and H. E. Katz, *Science*, 1995, **268**, 270–271.
25 F. Dinelli, M. Murgia, P. Levy, M. Cavallini, F. Biscarini and D. M. de Leeuw, *Phys. Rev. Lett.*, 2004, **92**, 116802.
26 T. Muck, V. Wagner, U. Bass, M. Leufgen, J. Geurts and L. W. Molenkamp, *Synth. Met.*, 2004, **146**, 317–320.
27 V. Coropceanu, J. r. m. Cornil, D. A. da Silva Filho, Y. Olivier, R. Silbey and J.-L. Br√©das, *Chem. Rev.*, 2007, **107**, 926–952.
28 H. Yan, Z. H. Chen, Y. Zheng, C. Newman, J. R. Quinn, F. Dotz, M. Kastler and A. Facchetti, *Nature*, 2009, **457**, 679–686.
29 A. L. Briseno, S. C. B. Mannsfeld, M. M. Ling, S. H. Liu, R. J. Tseng, C. Reese, M. E. Roberts, Y. Yang, F. Wudl and Z. N. Bao, *Nature*, 2006, **444**, 913–917.
30 T. Sekitani, M. Takamiya, Y. Noguchi, S. Nakano, Y. Kato, T. Sakurai and T. Someya, *Nat. Mater.*, 2007, **6**, 413–417.
31 A. Tracz, J. K. Jeszka, M. D. Watson, W. Pisula, K. Müllen and T. Pakula, *J. Am. Chem. Soc.*, 2003, **125**, 1682–1683.
32 X. L. Chen, Z. Bao, B. J. Sapjeta, A. J. Lovinger and B. Crone, *Adv. Mater.*, 2000, **12**, 344–347.
33 K. C. Dickey, J. E. Anthony and Y. L. Loo, *Adv. Mater.*, 2006, **18**, 1721–1726.

34 I. O. Shklyarevskiy, P. Jonkheijm, N. Stutzmann, D. Wasserberg, H. J. Wondergem, P. C. M. Christianen, A. P. H. J. Schenning, D. M. de Leeuw, Ž. Tomović, J. Wu, K. Müllen and J. C. Maan, *J. Am. Chem. Soc.*, 2005, **127**, 16233–16237.
35 J. Locklin, K. Shinbo, K. Onishi, F. Kaneko, Z. Bao and R. C. Advincula, *Chem. Mater.*, 2003, **15**, 1404–1412.
36 T. D. Anthopoulos, F. B. Kooistra, H. J. Wondergem, D. Kronholm, J. C. Hummelen and D. M. de Leeuw, *Adv. Mater.*, 2006, **18**, 1679–1684.
37 C.-Y. Liu and A. J. Bard, *Chem. Mater.*, 2000, **12**, 2353–2362.
38 Y. Ito, A. A. Virkar, S. Mannsfeld, J. H. Oh, M. Toney, J. Locklin and Z. Bao, *J. Am. Chem. Soc.*, 2009, **131**, 9396–9404.
39 Q. Tang, L. Jiang, Y. Tong, H. Li, Y. Liu, Z. Wang, W. Hu, Y. Liu and D. Zhu, *Adv. Mater.*, 2008, **20**, 2947–2951.
40 R. J. Li, W. P. Hu, Y. Q. Liu and D. B. Zhu, *Acc. Chem. Res.*, 2010, **43**, 529–540.
41 L. Jiang, H. Dong and W. Hu, *J. Mater. Chem.*, 2010, **20**, 4994–5007.
42 C. Reese and Z. Bao, *Mater. Today*, 2007, **10**, 20–27.
43 D. Braga and G. Horowitz, *Adv. Mater.*, 2009, **21**, 1473–1486.
44 L. Jiang, H. Dong, Q. Meng, H. Li, M. He, Z. Wei, Y. He and W. Hu, *Adv. Mater.*, 2011, **23**, 2059–2063.
45 K. Nakayama, Y. Hirose, J. Soeda, M. Yoshizumi, T. Uemura, M. Uno, W. Li, M. J. Kang, M. Yamagishi, Y. Okada, E. Miyazaki, Y. Nakazawa, A. Nakao, K. Takimiya and J. Takeya, *Adv. Mater.*, 2011, **23**, 1626–1629.
46 K. Takimiya, H. Ebata, K. Sakamoto, T. Izawa, T. Otsubo and Y. Kunugi, *J. Am. Chem. Soc.*, 2006, **128**, 12604–12605.
47 H. Meng, F. Sun, M. B. Goldfinger, F. Gao, D. J. Londono, W. J. Marshal, G. S. Blackman, K. D. Dobbs and D. E. Keys, *J. Am. Chem. Soc.*, 2006, **128**, 9304–9305.
48 H. Klauk, U. Zschieschang, R. T. Weitz, H. Meng, T. Sun, G. Nunes, D. E. Keys, C. R. Fincher and Z. Xiang, *Adv. Mater.*, 2007, **19**, 3882–3887.
49 L. Zhang, L. Tan, Z. Wang, W. Hu and D. Zhu, *Chem. Mater.*, 2009, **21**, 1993–1999.
50 L. Q. Li, Q. X. Tang, H. X. Li, X. D. Yang, W. P. Hu, Y. B. Song, Z. G. Shuai, W. Xu, Y. Q. Liu and D. B. Zhu, *Adv. Mater.*, 2007, **19**, 2613–2617.
51 C.-a. Di, G. Yu, Y. Liu, Y. Guo, X. Sun, J. Zheng, Y. Wen, Y. Wang, W. Wu and D. Zhu, *Phys. Chem. Chem. Phys.*, 2009, **11**, 7268–7273.
52 D. J. Gundlach, Y. Y. Lin, T. N. Jackson, S. F. Nelson and D. G. Schlom, *IEEE Electron Device Lett.*, 1997, **18**, 87–89.
53 M. Burghard, H. Klauk and K. Kern, *Adv. Mater.*, 2009, **21**, 2586–2600.
54 B. Stevens, S. R. Perez and J. A. Ors, *J. Am. Chem. Soc.*, 1974, **96**, 6846–6850.
55 J. G. Laquindanum, H. E. Katz and A. J. Lovinger, *J. Am. Chem. Soc.*, 1998, **120**, 664–672.
56 F. De Angelis, M. Gaspari, A. Procopio, G. Cuda and E. Di Fabrizio, *Chem. Phys. Lett.*, 2009, **468**, 193–196.
57 L. B. Roberson, J. Kowalik, L. M. Tolbert, C. Kloc, R. Zeis, X. Chi, R. Fleming and C. Wilkins, *J. Am. Chem. Soc.*, 2005, **127**, 3069–3075.
58 F. De Angelis, S. Cipolloni, L. Mariucci and G. Fortunato, *Appl. Phys. Lett.*, 2006, **88**, 193508.
59 K. Takimiya, Y. Konda, H. Ebata, N. Niihara and T. Otsubo, *J. Org. Chem.*, 2005, **70**, 10569–10571.
60 O. D. Jurchescu, J. Baas and T. T. M. Palstra, *Appl. Phys. Lett.*, 2004, **84**, 3061–3063.
61 T. W. Kelley, D. V. Muyres, P. F. Baude, T. P. Smith and T. D. Jones, *Mat. Res. Soc. Symp. Proc.*, 2003, **771**, 169–179.
62 T. W. Kelley, L. D. Boardman, T. D. Dunbar, D. V. Muyres, M. J. Pellerite and T. Y. P. Smith, *J. Phys. Chem. B*, 2003, **107**, 5877–5881.
63 T. W. Kelley, P. F. Baude, C. Gerlach, D. E. Ender, D. Muyres, M. A. Haase, D. E. Vogel and S. D. Theiss, *Chem. Mater.*, 2004, **16**, 4413–4422.
64 C.-H. Wang, C.-Y. Hsieh and J.-C. Hwang, *Adv. Mater.*, 2011, **23**, 1630–1634.
65 H. Okamoto, N. Kawasaki, Y. Kaji, Y. Kubozono, A. Fujiwara and M. Yamaji, *J. Am. Chem. Soc.*, 2008, **130**, 10470–10471.
66 O. Kwon, V. Coropceanu, N. E. Gruhn, J. C. Durivage, J. G. Laquindanum, H. E. Katz, J. Cornil and J. L. Bredas, *J. Chem. Phys.*, 2004, **120**, 8186–8194.
67 M. M. Payne, S. R. Parkin, J. E. Anthony, C. C. Kuo and T. N. Jackson, *J. Am. Chem. Soc.*, 2005, **127**, 4986–4987.
68 P. Zhu, H. Kang, A. Facchetti, G. Evmenenko, P. Dutta and T. J. Marks, *J. Am. Chem. Soc.*, 2003, **125**, 11496–11497.
69 A. N. Sokolov, T. Friščić and L. R. MacGillivray, *J. Am. Chem. Soc.*, 2006, **128**, 2806–2807.
70 S. Subramanian, S. K. Park, S. R. Parkin, V. Podzorov, T. N. Jackson and J. E. Anthony, *J. Am. Chem. Soc.*, 2008, **130**, 2706–2707.
71 M. Fourmigué and P. Batail, *Chem. Rev.*, 2004, **104**, 5379–5418.
72 K. Reichenbacher, H. I. Suss and J. Hulliger, *Chem. Soc. Rev.*, 2005, **34**, 22–30.
73 P. Metrangolo, G. Resnati, T. Pilati, R. Liantonio and F. Meyer, *J. Polym. Sci., Part A: Polym. Chem.*, 2007, **45**, 1–15.
74 G. W. Coates, A. R. Dunn, L. M. Henling, J. W. Ziller, E. B. Lobkovsky and R. H. Grubbs, *J. Am. Chem. Soc.*, 1998, **120**, 3641–3649.
75 M. L. Tang, A. D. Reichardt, T. Siegrist, S. C. B. Mannsfeld and Z. N. Bao, *Chem. Mater.*, 2008, **20**, 4669–4676.
76 K. Takimiya, Y. Kunugi, Y. Konda, N. Niihara and T. Otsubo, *J. Am. Chem. Soc.*, 2004, **126**, 5084–5085.
77 J. H. Gao, L. Q. Li, Q. Meng, R. J. Li, H. Jiang, H. X. Li and W. P. Hu, *J. Mater. Chem.*, 2007, **17**, 1421–1426.
78 Y. Didane, G. H. Mehl, A. Kumagai, N. Yoshimoto, C. Videlot-Ackermann and H. Brisset, *J. Am. Chem. Soc.*, 2008, **130**, 17681–17683.
79 H. Meng, F. Sun, M. B. Goldfinger, G. D. Jaycox, Z. Li, W. J. Marshall and G. S. Blackman, *J. Am. Chem. Soc.*, 2005, **127**, 2406–2407.
80 M.-C. Um, J. Jang, J. Kang, J.-P. Hong, D. Y. Yoon, S. H. Lee, J.-J. Kim and J.-I. Hong, *J. Mater. Chem.*, 2008, **18**, 2234–2239.
81 C. L. Wang, Z. M. Wei, Q. Meng, H. P. Zhao, W. Xu, H. X. Li and W. P. Hu, *Org. Electron.*, 2010, **11**, 544–551.
82 L. Tan, L. Zhang, X. Jiang, X. Yang, L. Wang, Z. Wang, L. Li, W. Hu, Z. Shuai, L. Li and D. Zhu, *Adv. Funct. Mater.*, 2009, **19**, 272–276.
83 H. Dong, C. Wang and W. Hu, *Chem. Commun.*, 2010, **46**, 5211–5222.
84 H. Ebata, T. Izawa, E. Miyazaki, K. Takimiya, M. Ikeda, H. Kuwabara and T. Yui, *J. Am. Chem. Soc.*, 2007, **129**, 15732–15733.
85 T. Izawa, E. Miyazaki and K. Takimiya, *Adv. Mater.*, 2008, **20**, 3388–3392.
86 T. Yamamoto and K. Takimiya, *J. Am. Chem. Soc.*, 2007, **129**, 2224–2225.
87 M. J. Kang, I. Doi, H. Mori, E. Miyazaki, K. Takimiya, M. Ikeda and H. Kuwabara, *Adv. Mater.*, 2011, **23**, 1222–1225.
88 S. T. Bromley, M. Mas-Torrent, P. Hadley and C. Rovira, *J. Am. Chem. Soc.*, 2004, **126**, 6544–6545.
89 A. Marrocchi, M. Seri, C. Kim, A. Facchetti, A. Taticchi and T. J. Marks, *Chem. Mater.*, 2009, **21**, 2592–2594.
90 Q. Meng, J. H. Gao, R. J. Li, L. Jiang, C. L. Wang, H. P. Zhao, C. M. Liu, H. X. Li and W. P. Hu, *J. Mater. Chem.*, 2009, **19**, 1477–1482.
91 F. Silvestri, A. Marrocchi, M. Seri, C. Kim, T. J. Marks, A. Facchetti and A. Taticchi, *J. Am. Chem. Soc.*, 2010, **132**, 6108–6123.
92 C. L. Wang, Y. L. Liu, Z. Y. Ji, E. J. Wang, R. J. Li, H. Jiang, Q. X. Tang, H. X. Li and W. P. Hu, *Chem. Mater.*, 2009, **21**, 2840–2845.
93 Q. Meng, L. Jiang, Z. Wei, C. Wang, H. Zhao, H. Li, W. Xu and W. Hu, *J. Mater. Chem.*, 2010, **20**, 10931–10935.
94 M. Kanno, Y. Bando, T. Shirahata, J. I. Inoue, H. Wada and T. Mori, *J. Mater. Chem.*, 2009, **19**, 6548–6555.
95 K. Y. Law, *Chem. Rev.*, 1993, **93**, 449–486.
96 H. B. Wang, D. Song, J. L. Yang, B. Yu, Y. H. Geng and D. H. Yan, *Appl. Phys. Lett.*, 2007, **90**, 253510.
97 W. Pisula, A. Menon, M. Stepputat, I. Lieberwirth, U. Kolb, A. Tracz, H. Sirringhaus, T. Pakula and K. Müllen, *Adv. Mater.*, 2005, **17**, 684–689.
98 S. Ando, R. Murakami, J. Nishida, H. Tada, Y. Inoue, S. Tokito and Y. Yamashita, *J. Am. Chem. Soc.*, 2005, **127**, 14996–14997.
99 D. Kumaki, S. Ando, S. Shimono, Y. Yamashita, T. Umeda and S. Tokito, *Appl. Phys. Lett.*, 2007, **90**, 053506.

100 D. Shukla, S. F. Nelson, D. C. Freeman, M. Rajeswaran, W. G. Ahearn, D. M. Meyer and J. T. Carey, *Chem. Mater.*, 2008, **20**, 7486–7491.
101 R. J. Chesterfield, J. C. McKeen, C. R. Newman, P. C. Ewbank, D. A. da Silva, J. L. Bredas, L. L. Miller, K. R. Mann and C. D. Frisbie, *J. Phys. Chem. B*, 2004, **108**, 19281–19292.
102 S. Tatemichi, M. Ichikawa, T. Koyama and Y. Taniguchi, *Appl. Phys. Lett.*, 2006, **89**, 112108.
103 S. Kobayashi, T. Takenobu, S. Mori, A. Fujiwara and Y. Iwasa, *Appl. Phys. Lett.*, 2003, **82**, 4581.
104 C. Waldauf, P. Schilinsky, M. Perisutti, J. Hauch and C. J. Brabec, *Adv. Mater.*, 2003, **15**, 2084–2088.
105 M. Chikamatsu, S. Nagamatsu, Y. Yoshida, K. Saito, K. Yase and K. Kikuchi, *Appl. Phys. Lett.*, 2005, **87**, 203504.
106 K. Itaka, M. Yamashiro, J. Yamaguchi, M. Haemori, S. Yaginuma, Y. Matsumoto, M. Kondo and H. Koinuma, *Adv. Mater.*, 2006, **18**, 1713–1716.
107 T. D. Anthopoulos, B. Singh, N. Marjanovic, N. S. Sariciftci, A. M. Ramil, H. Sitter, M. Colle and D. M. d. Leeuw, *Appl. Phys. Lett.*, 2006, **89**, 213504.
108 Z. Liang, Q. Tang, J. Xu and Q. Miao, *Adv. Mater.*, 2011, **23**, 1535–1539.
109 X. K. Gao, C. A. Di, Y. B. Hu, X. D. Yang, H. Y. Fan, F. Zhang, Y. Q. Liu, H. X. Li and D. B. Zhu, *J. Am. Chem. Soc.*, 2010, **132**, 3697–3699.
110 Y. Zhao, C.-a. Di, X. Gao, Y. Hu, Y. Guo, L. Zhang, Y. Liu, J. Wang, W. Hu and D. Zhu, *Adv. Mater.*, 2011, **23**, 2448–2453.
111 H. E. Katz, A. J. Lovinger, J. Johnson, C. Kloc, T. Siegrist, W. Li, Y. Y. Lin and A. Dodabalapur, *Nature*, 2000, **404**, 478–481.
112 B. J. Jung, J. Sun, T. Lee, A. Sarjeant and H. E. Katz, *Chem. Mater.*, 2009, **21**, 94–101.
113 K. C. See, C. Landis, A. Sarjeant and H. E. Katz, *Chem. Mater.*, 2008, **20**, 3609–3616.
114 R. J. Chesterfield, J. C. McKeen, C. R. Newman, P. C. Ewbank, D. A. da Silva Filho, J.-L. Brédas, L. L. Miller, K. R. Mann and C. D. Frisbie, *J. Phys. Chem. B*, 2004, **108**, 19281–19292.
115 H. Z. Chen, M. M. Ling, X. Mo, M. M. Shi, M. Wang and Z. Bao, *Chem. Mater.*, 2007, **19**, 816–824.
116 B. A. Jones, A. Facchetti, T. J. Marks and M. R. Wasielewski, *Chem. Mater.*, 2007, **19**, 2703–2705.
117 B. A. Jones, M. J. Ahrens, M.-H. Yoon, A. Facchetti, T. J. Marks and M. R. Wasielewski, *Angew. Chem., Int. Ed.*, 2004, **43**, 6363–6366.
118 B. Yoo, T. Jung, D. Basu, A. Dodabalapur, B. A. Jones, A. Facchetti, M. R. Wasielewski and T. J. Marks, *Appl. Phys. Lett.*, 2006, **88**, 082104.
119 A. S. Molinari, H. Alves, Z. Chen, A. Facchetti and A. F. Morpurgo, *J. Am. Chem. Soc.*, 2009, **131**, 2462–2463.
120 R. Schmidt, J. H. Oh, Y.-S. Sun, M. Deppisch, A.-M. Krause, K. Radacki, H. Braunschweig, M. Könemann, P. Erk, Z. Bao and F. Würthner, *J. Am. Chem. Soc.*, 2009, **131**, 6215–6228.
121 M. M. Ling, P. Erk, M. Gomez, M. Koenemann, J. Locklin and Z. N. Bao, *Adv. Mater.*, 2007, **19**, 1123–1127.